Adaptive Neuro-Wavelet Control for Switching Power Supplies

Chih-Min Lin, *Senior Member, IEEE*, Kun-Neng Hung, and Chun-Fei Hsu, *Member, IEEE*

***Abstract*—The switching power supplies can convert one level of electrical voltage into another level by switching action. They are very popular because of their high efficiency and small size. This paper proposes an adaptive neuro-wavelet (ANW) control system for the switching power supplies. In the ANW control system, a neural controller is the main controller used to mimic an ideal controller and a compensated controller is designed to recover the residual of the approximation error. In this study, an online adaptive law with a variable optimal learning-rate is derived based on the Lyapunov stability theorem, so that not only the stability of the system can be guaranteed but also the convergence of controller parameters can be speeded up. Then, the proposed ANW control system is applied to control a forward switching power supply. Experimental results show that the proposed ANW controller can achieve favorable regulation performance for the switching power supply even under input voltage and load resistance variations.**

***Index Terms*—Adaptive control, Lyapunov stability theorem, optimal learning-rate, switching power supply, wavelet neural network (WNN).**

I. Introduction

RECENTLY, the neural-network-based control technique has represented an alternative design method for various control systems [1]–[5]. The successful key element is the approximation ability, where the parameterized neural network can approximate an unknown system dynamics through learning. Wavelets have been combined with the neural network to create wavelet neural networks (WNNs). The training algorithms for WNN typically converge in a smaller number of iterations than the conventional neural networks [6]–[8]. Unlike the sigmoid functions used in conventional neural networks, the second layer of WNN is a wavelet form, in which the translation and dilation parameters are included. Thus, WNN has been proved to be better than the other neural networks in that the structure can provide more potential to enrich the mapping relationship between inputs and outputs [8]. There has been considerable interest in exploring the applications of WNN to deal with nonlinearity and uncertainties of real-time servo control systems [9]–[12]. These WNN-based controllers combine the capability of artificial neural networks for learning ability and the capability of wavelet decomposition for identification ability. Thus, the WNN-based control systems have been adopted widely for the closed-loop control of complex dynamical systems owing to its fast learning property and good generalization capability [9], [10].

Due to the rapid development of power semiconductor devices in personal computers, computer peripherals, and adapters, the switching power supplies are popular in modern industrial applications. To obtain high quality power systems, the popular control technique of the switching power supplies is the pulsewidth modulation (PWM) approach [13], [14]. By varying the duty ratio of the PWM modulator, the switching power supply can convert one level of electrical voltage into the desired level. From the control viewpoint, the controller design of the switching power supply is an intriguing issue, which must cope with wide input voltage and load resistance variations to ensure the stability in any operating condition while providing fast transient response. Over the past decade, there have been many different approaches proposed for PWM switching control design based on PI control [15], optimal control [16], sliding-mode control [17], [18], fuzzy control [17], [19], and adaptive control [20] techniques. However, most of these approaches require the time-consuming trial-and-error tuning procedure to achieve satisfactory performance; some of them can not achieve satisfactory performance under the changes of operating point; and some of them have not given the stability analysis.

The motivation of this paper is to design an adaptive neuro-wavelet (ANW) control system for the switching power supply. The proposed ANW control system is comprised of a neural controller and a compensated controller. The neural controller using a WNN is designed to mimic an ideal controller and a compensated controller is designed to compensate for the approximation error between the ideal controller and the neural controller. The online adaptive laws are derived based on the Lyapunov stability theorem so that the stability of the system can be guaranteed. Finally, the proposed ANW control scheme is applied to control a forward switching power supply. The experimental results demonstrate that the proposed ANW control scheme can achieve favorable control performance, even the switching power supply is subject to the input voltage and load resistance variations.

II. Problem Formulation

The switching power supplies can convert one level of electrical voltage into another level by switching action. Nowadays, they are very popular because of its high efficiency and small size [13]. Among the various switching control methods, PWM which is based on fast switching and duty ratio control is the

Manuscript received September 9, 2005; revised March 28, 2006. This work was supported in part by the National Science Council of Taiwan, R.O.C. under Grant NSC 93-2213-E-155-038.

C.-M. Lin and K.-N. Hung are with the Department of Electrical Engineering, Yuan-Ze University, Taoyuan 320, Taiwan, R.O.C. (e-mail: cml@saturn.yzu.edu.tw; s937102@mail.yzu.edu.tw).

C.-F. Hsu is with the Department of Electrical and Control Engineering, National Chiao-Tung University, Hsinchu 300, Taiwan, R.O.C. (e-mail: fei@cn.nctu.edu.tw).

Color versions of one or more of the figures in this paper are available online at http://ieeexplore.ieee.org.

Digital Object Identifier 10.1109/TPEL.2006.886630

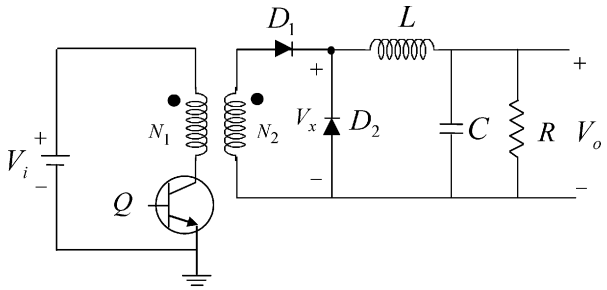

Fig. 1. Forward switching power supply.

most widely considered one. The switching frequency is constant and the duty cycle, $d(N)$, varies with the load resistance variations at the Nth sampling time. The output of the designed controller, $\delta d(N)$, is the change of duty cycle. Then, the duty cycle is determined by adding the previous duty cycle $d(N-1)$ to the change of duty cycle $\delta d(N)$, i.e.

$$d(N) = d(N-1) + \delta d(N). \tag{1}$$

This duty cycle signal is then sent to a PWM output stage that generates the appropriate switching pattern for the switching power supplies. In this paper, a forward switching power supply is discussed as shown in Fig. 1, where V_i and V_o are the input and output voltages of the converter, respectively, D_1 and D_2 are the diodes, L is the inductor, C is the output capacitor, R is the resistor, and Q is the transistor which control the converter circuit operating in different modes. When the transistor is ON, V_i appears across the primary and then generates

$$V_x = \frac{N_2}{N_1}(V_i - V_{\text{lost}}) \tag{2}$$

where N_1 is the turns of primary power winding, N_2 is the turns of slave power winding, and V_{lost} denotes the voltage drop occurring by transistor and diodes and represents the unmodeled dynamics in practical applications. The diode D_1 on the secondary ensures that only positive voltages are applied to the output circuit while diode D_2 provides a circulating path for inductor current. By the averaging method, the output voltage can be expressed as [13]

$$V_o = \frac{N_2}{N_1}(V_i - V_{\text{lost}})d. \tag{3}$$

Since N_1, N_2, and $V_i - V_{\text{lost}}$ are considered as constants, differentiating both sides of (3) with respect to time yields

$$\dot{V}_o = \frac{N_2}{N_1}(V_i - V_{\text{lost}})\delta d = gu \tag{4}$$

where $g \equiv (N_2/N_1)(V_i - V_{\text{lost}})$ is the control gain which is a positive constant and $u \equiv \delta d$ is the controller output. The control problem of forward switching power supplies is to control the change of duty cycle δd so that the output voltage V_o can provide a fixed voltage under the occurrence of the uncertainties such as the wide input voltages and load variations. The output error voltage is defined as

$$e = V_{\text{ref}} - V_o \tag{5}$$

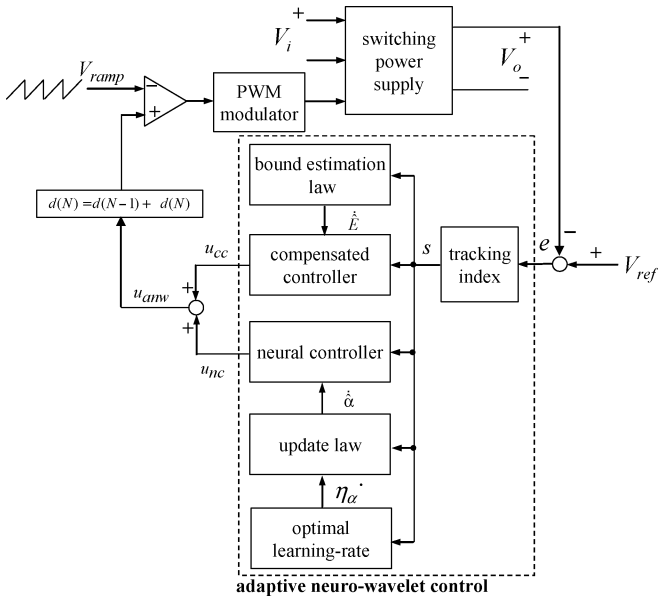

Fig. 2. Block diagram of the ANW control for switching power supply.

where V_{ref} is the output reference voltage. The control law of the duty cycle is determined by the error voltage signal to provide fast transient response and small overshoot in the output voltage. If the system parameters are well known, an ideal controller can be designed as

$$u^* = g^{-1}(\dot{V}_{\text{ref}} + ke). \tag{6}$$

If k is chosen to correspond to the coefficients of a Hurwitz polynomial, that is a polynomial whose roots lie strictly in the open left half of the complex plane, then $\lim_{t\to\infty} e = 0$. Since the system parameters may be unknown or perturbed, the ideal controller u^* in (6) can not be precisely implemented.

III. Design of Adaptive Neuro-Wavelet Control

In order to efficiently control the output voltage of the switching power supplies, an ANW control system shown in Fig. 2 is introduced. The configuration of the ANW control system consists of a neural controller and a compensated controller, i.e.

$$u_{anw} = u_{nc} + u_{cc} \tag{7}$$

where u_{nc} is the neural controller and u_{cc} is the compensated controller. The neural controller uses a WNN to mimic the ideal controller and the compensated controller is designed to compensate for the difference between the ideal controller and the neural controller. Substituting (7) into (4), we get

$$\dot{V}_o = g(u_{nc} + u_{cc}). \tag{8}$$

The error equation governing the system can be obtained by combining (6) and (8), i.e.

$$\dot{e} + ke = g(u^* - u_{nc} - u_{cc}). \tag{9}$$

A. Wavelet Neural Network

A four-layer WNN shown in Fig. 3, which comprises an input layer (the i layer), a mother wavelet layer (the j layer), a wavelet layer (the k layer), and an output layer (the o layer), is adopted to implement the neural controller. The signal propagation and the basic function in each layer are now introduced. In this subsection, the superscript denotes the number of layer. For every node i in the input layer, the net input and the net output are represented as follows.

Layer 1: Input Layer:

$$net_i^1 = x_i^1 \tag{10}$$

$$y_i^1 = f_i^1\left(net_i^1\right) = net_i^1, \quad i = 1, 2, \ldots, n_L. \tag{11}$$

Layer 2: Wavelet Layer:

A family of wavelets is constructed by translations and dilations performed on the mother wavelet. In the mother wavelet layer each node performs a wavelet ϕ_j that is derived from its mother wavelet. For the jth node

$$net_j^2 = \frac{x_i^2 - m_{ij}}{\sigma_{ij}} \tag{12}$$

$$y_j^2 = f_j^2\left(net_j^2\right) = \phi_j\left(net_j^2\right), \quad j = 1, 2, \ldots, n_M \tag{13}$$

where m_{ij} and σ_{ij} are, respectively, the translation and dilation in the jth term of the ith input x_i^2 to the node of mother wavelet layer and n_M is the total number of the wavelets with respect to the input nodes.

Layer 3: Inference Layer:

Each node k in the wavelet layer is denoted by $\prod$, which multiplies the input signals and outputs the result of the product, i.e., the product of j mono-dimensional wavelets with respect to the input node. For the kth rule node

$$net_k^3 = \prod_j^{n_M} x_j^3 \tag{14}$$

$$y_k^3 = f_k^3\left(net_k^3\right) = net_k^3, \quad k = 1, 2, \ldots, n_N \tag{15}$$

where x_j^3 represents the jth input to the node of wavelet layer and n_N is the number of wavelets.

Layer 4: Output Layer:

The single node o in the output layer is labelled as Σ, which computes the overall output as the summation of all input signals

$$net_o^4 = \sum_k^{n_N} \alpha_k^4 \cdot x_k^4 \tag{16}$$

$$y_o^4 = f_o^4\left(net_o^4\right) = net_o^4 \tag{17}$$

where the connecting weight α_k^4 is the output action strength of the kth output associated with the kth wavelet and x_k^4 represents the kth input to the node of output layer.

There are many kinds of wavelets that can be used in WNN. In this paper, the Gaussian wavelet function $\phi(x) = \cos(\omega x)\exp(-x^2)$ is selected as a mother wavelet and one can take direct products of such scalar wavelets in the multidimensional case in which ω is the frequency. Define the vectors σ and m collecting all parameter of hidden layer in WNN as

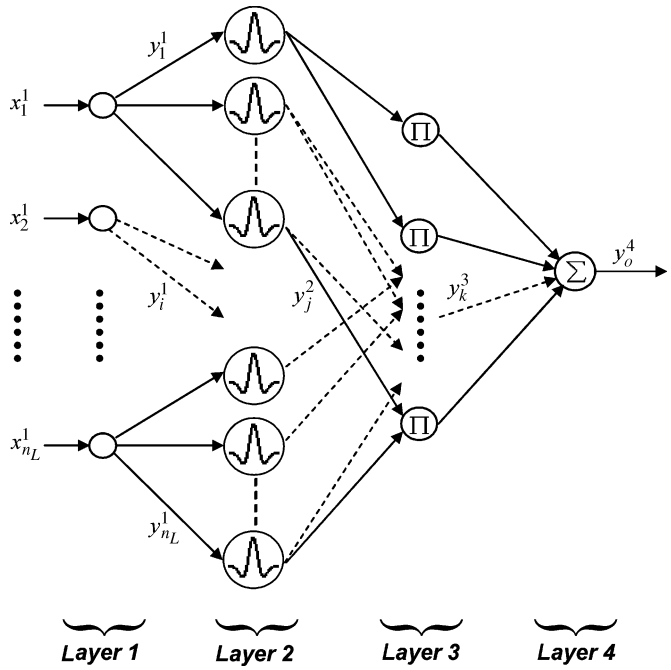

Fig. 3. Structure of wavelet neural network.

$$\sigma = [\sigma_{11} \cdots \sigma_{n_M 1} \sigma_{12} \cdots \sigma_{n_M 2} \cdots \sigma_{1 n_M} \cdots \sigma_{n_M n_N}]^T \tag{18}$$

$$m = [m_{11} \cdots m_{n_M 1} m_{12} \cdots m_{n_M 2} \cdots m_{1 n_N} \cdots m_{n_M n_N}]^T \tag{19}$$

Then the output of the WNN can be represented in a vector form

$$y_o^4(x, \sigma, m, \alpha) = \alpha^T \Theta(x, \sigma, m) \tag{20}$$

where $x = [x_1^1, x_2^1, \ldots, x_{n_L}^1]^T$, $\alpha = [\alpha_1, \alpha_2, \ldots, \alpha_{n_N}]^T$, and $\Theta = [\Theta_1, \Theta_2, \ldots, \Theta_{n_N}]^T = [x_1^4, x_2^4, \ldots, x_{n_N}^4]^T$.

B. Control System Design

The neural controller is designed to estimate the ideal controller in (6). By the universal approximation theorem [21], there exists an optimal neural controller u_{nc}^* such that

$$u^* = u_{nc}^* + \varepsilon \equiv \alpha^{*T}\Theta + \varepsilon \tag{21}$$

where ε is a minimum approximation error and α^* is the optimal parameter vector of α. The approximation error ε is assumed to be bounded by a positive constant E (i.e., $|\varepsilon| < E$). This approximation error bound E is generally unobtainable in practical applications, so that it will be estimated in the following derivations. Moreover, the optimal neural controller u_{nc}^* can not be obtained, so that an online estimation neural controller is defined as

$$u_{nc} = \hat{\alpha}^T \Theta \tag{22}$$

where $\hat{\alpha}$ is an estimate of the optimal parameter vector α^*. Define the estimation error $\tilde{u}$ as

$$\tilde{u} = u^* - u_{nc} = \alpha^{*T}\Theta + \varepsilon - \hat{\alpha}^T\Theta = \tilde{\alpha}^T\Theta + \varepsilon \tag{23}$$

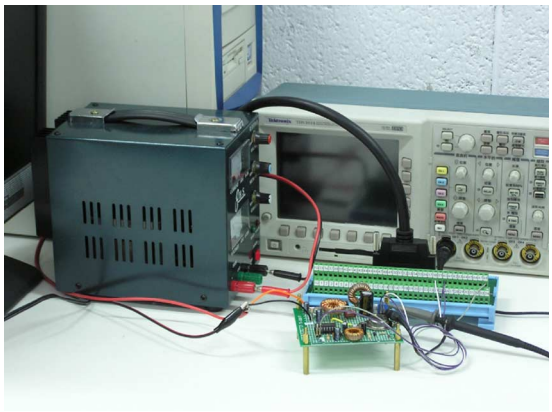

Fig. 4. Snapshot of the experiment setup.

where $\widetilde{\alpha} = \alpha^* - \hat{\alpha}$. Define a tracking index as

$$s = e + k\int_0^t e d\tau \tag{24}$$

which is the input of the neural network. Then, the error (9) can be rewritten as

$$\dot{s} = g(\widetilde{\alpha}^T\Theta + \varepsilon - u_{cc}). \tag{25}$$

To relax the requirement of the uncertain bound E, a bound estimation mechanism is developed to observe the bound of the approximation error. Define the estimation error of the bound

$$\widetilde{E} = E - \hat{E} \tag{26}$$

where $\hat{E}$ is the estimated error bound. To guarantee the stability of the adaptive neuro-wavelet control approach, a Lyapunov function candidate is defined as

$$V_1(s,\widetilde{\alpha},\widetilde{E}) = \frac{1}{2}s^2 + \frac{g}{2\eta_\alpha}\widetilde{\alpha}^T\widetilde{\alpha} + \frac{g}{2\eta_E}\widetilde{E}^2 \tag{27}$$

where η_E is a constant learning-rate, and η_α is a variable learning-rate, which will be discussed in the following subsection to speed up the convergence of controller parameter. Differentiating (27) with respect to time and using (25), we get

$$\begin{aligned}\dot{V}_1(s,\widetilde{\alpha},\widetilde{E}) &= s\dot{s} + \frac{g}{\eta_\alpha}\widetilde{\alpha}^T\dot{\widetilde{\alpha}} - \frac{g}{2\eta_\alpha^2}\widetilde{\alpha}^T\widetilde{\alpha}\dot{\eta}_\alpha + \frac{g}{\eta_E}\widetilde{E}\dot{\widetilde{E}}\\ &= sg(\widetilde{\alpha}^T\Theta + \varepsilon - u_{cc}) + \frac{g}{\eta_\alpha}\widetilde{\alpha}^T\dot{\widetilde{\alpha}}\\ &\quad - \frac{g}{2\eta_\alpha^2}\widetilde{\alpha}^T\widetilde{\alpha}\dot{\eta}_\alpha + \frac{g}{\eta_E}\widetilde{E}\dot{\widetilde{E}}\\ &= g\widetilde{\alpha}^T\left(s\Theta + \frac{\dot{\widetilde{\alpha}}}{\eta_\alpha} - \tau\right) + sg(\varepsilon - u_{cc})\\ &\quad + \frac{g}{\eta_E}\widetilde{E}\dot{\widetilde{E}} - \frac{g}{2\eta_\alpha^2}\widetilde{\alpha}^T\widetilde{\alpha}\dot{\eta}_\alpha\end{aligned} \tag{28}$$

where $\tau = \widetilde{\alpha}\dot{\eta}_\alpha/2\eta_\alpha^2$. For achieving $\dot{V}_1 \le 0$, the adaptive laws and the compensated controller are chosen as

$$u_{cc} = \hat{E}\mathrm{sgn}(s)\mathrm{sgn}(g) = \hat{E}\mathrm{sgn}(s) \tag{29}$$

$$\dot{\widetilde{\alpha}} = -\dot{\hat{\alpha}} = -\eta_\alpha(s\Theta - \tau) \tag{30}$$

$$\dot{\widetilde{E}} = -\dot{\hat{E}} = -\eta_E|s|\mathrm{sgn}(g) = -\eta_E|s| \tag{31}$$

where $\mathrm{sgn}(\cdot)$ is a sign function. Then (28) can be rewritten as

$$\begin{aligned}\dot{V}_1(s,\widetilde{\alpha},\widetilde{E}) &= \varepsilon sg - \hat{E}|s||g| - (E - \hat{E})|s||g|\\ &\le |\varepsilon||s||g| - E|s||g|\\ &= -(E - |\varepsilon|)|s||g| \le 0.\end{aligned} \tag{32}$$

Since $\dot{V}_1(s,\widetilde{\alpha},\widetilde{E})$ is negative semidefinite, that is $V_1(s(t),\widetilde{\alpha}(t),\widetilde{E}(t)) \le V_1(s(0),\widetilde{\alpha}(0),\widetilde{E}(0))$, it implies that s, $\widetilde{\alpha}$, and $\widetilde{E}$ are bounded. Let function $\Omega(t) \equiv (E - |\varepsilon|)sg \le (E - |\varepsilon|)|s||g| \le -\dot{V}_1$, and integrate $\Omega(t)$ with respect to time, then it is obtained that

$$\int_0^t \Omega(\tau)d\tau \le V_1\left(s(0),\widetilde{\alpha}(0),\widetilde{E}(0)\right) - V_1\left(s(t),\widetilde{\alpha}(t),\widetilde{E}(t)\right). \tag{33}$$

Because $V_1(s(0),\widetilde{\alpha}(0),\widetilde{E}(0))$ is bounded, and $V_1(s(t),\widetilde{\alpha}(t),\widetilde{E}(t))$ is nonincreasing and bounded, the following result can be obtained:

$$\lim_{t\to\infty}\int_0^t \Omega(\tau)d\tau < \infty. \tag{34}$$

Moreover, since $\dot{\Omega}(t)$ is bounded, by Barbalat's Lemma [22], $\lim_{t\to\infty}\Omega(t) = 0$. That is, $s \to 0$ as $t \to \infty$. As a result, the stability of the proposed adaptive neuro-wavelet system can be guaranteed.

C. Convergence Analyses

The adaptive law shown in (30) calls for a proper choice of the learning-rate η_α. For a small value of learning-rate, the convergence of controller parameter can be guaranteed but the convergent speed is very slow. On the other hand, if the learning-rate is too large, the parameter convergence may become more unstable. In order to train the WNN efficiently, an optimal learning-rate will be derived to achieve the fast convergence of output tracking error. First, the adaptive law shown in (30) can be rewritten as

$$\dot{\hat{\alpha}}_k = \eta_\alpha s x_k^4. \tag{35}$$

The central part of the training algorithm for a WNN concerns how to obtain recursively a gradient vector in which each element in the training algorithm is defined as the derivative of an energy function with respect to a parameter of the network. This is done by means of the chain rule, and this method is generally referred to as the back-propagation learning rule, because the gradient vector is calculated in the direction opposite to the

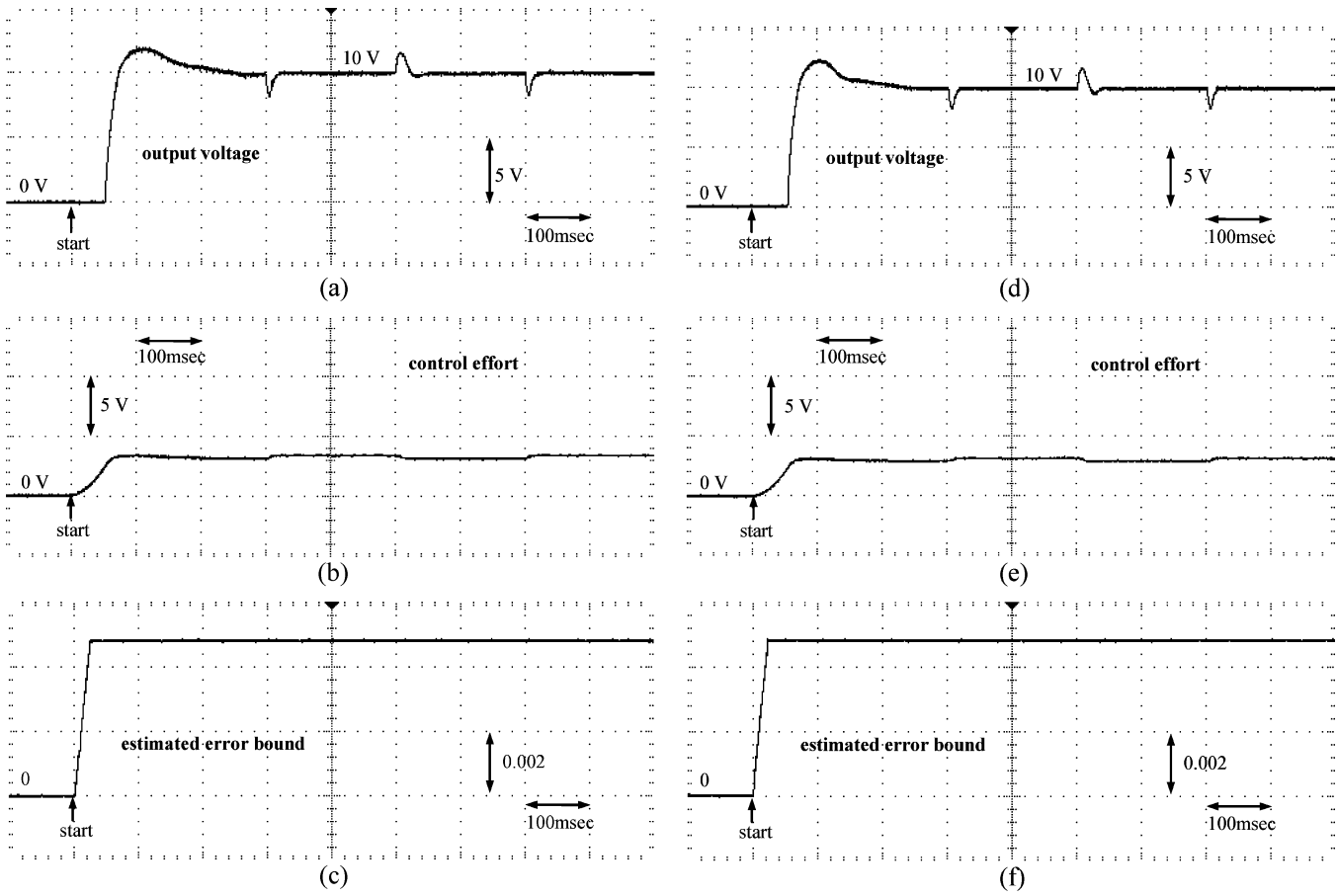

Fig. 5. Experimental results of ANW control with $\eta_\alpha = 0.0005$.

flow of the output of each node. In order to describe the online training algorithm of the WNN, a cost function is defined as

$$C = \frac{1}{2}e^2. \tag{36}$$

According to the gradient descent method, the adaptive law of the weight also can be represented as

$$\begin{aligned}\dot{\hat{\alpha}}_k &= -\eta_\alpha \frac{\partial C}{\partial \hat{\alpha}_k} \\ &= -\eta_\alpha \frac{\partial C}{\partial y_o^4}\frac{\partial y_o^4}{\partial net_o^4}\frac{\partial net_o^4}{\partial \hat{\alpha}_k} \\ &= -\eta_\alpha \frac{\partial C}{\partial y_o^4} x_k^4.\end{aligned} \tag{37}$$

Comparing (35) with (37), yields $(\partial C/\partial y_o^4) = -s$. Then, the convergence analysis in the following theorem is to derive specific learning-rate to assure convergence of the output tracking error.

Theorem 1: Let η_α be the learning-rate of the WNN output weights, and let $P_{\alpha\max}$ be defined as $P_{\alpha\max} \equiv \max_{n_N} \|P_\alpha(N)\|$, where $P_\alpha(N) = (\partial y_o^4/\partial \alpha_k^4)$ and $\|\cdot\|$ is the Euclidean norm in $\Re^n$. Then, the convergence of the output tracking error is guaranteed if η_α is chosen as

$$0 < \eta_\alpha < \frac{2}{(P_{\alpha\max})^2 \left[\frac{s}{e(N)}\right]^2}. \tag{38}$$

Moreover, the optimal learning-rate which achieves the fast convergence can be obtained as

$$\eta_\alpha^* = \frac{1}{(P_{\alpha\max})^2 \left[\frac{s}{e(N)}\right]^2}. \tag{39}$$

Proof: Since

$$P_\alpha(N) = \frac{\partial y_o^4}{\partial \alpha_k^4} = \frac{\partial\left(\sum_{k=1}^{n_N} \alpha_k^4 x_k^4\right)}{\partial \alpha_k^4} = x_k^4. \tag{40}$$

Then, a discrete-type Lyapunov function is selected as

$$V_2(N) = \frac{1}{2}e(N)^2. \tag{41}$$

The change in the Lyapunov function can be expressed as

$$\Delta V_2 = V_2(N+1) - V_2(N) = \frac{1}{2}\left[e(N+1)^2 - e(N)^2\right]. \tag{42}$$

Moreover, the error difference can be represented by

$$\begin{aligned}e(N+1) &= e(N) + \Delta e(N) \\ &= e(N) + \left[\frac{\partial e(N)}{\partial \alpha_k^4}\right]^T \Delta \alpha_k^4\end{aligned} \tag{43}$$

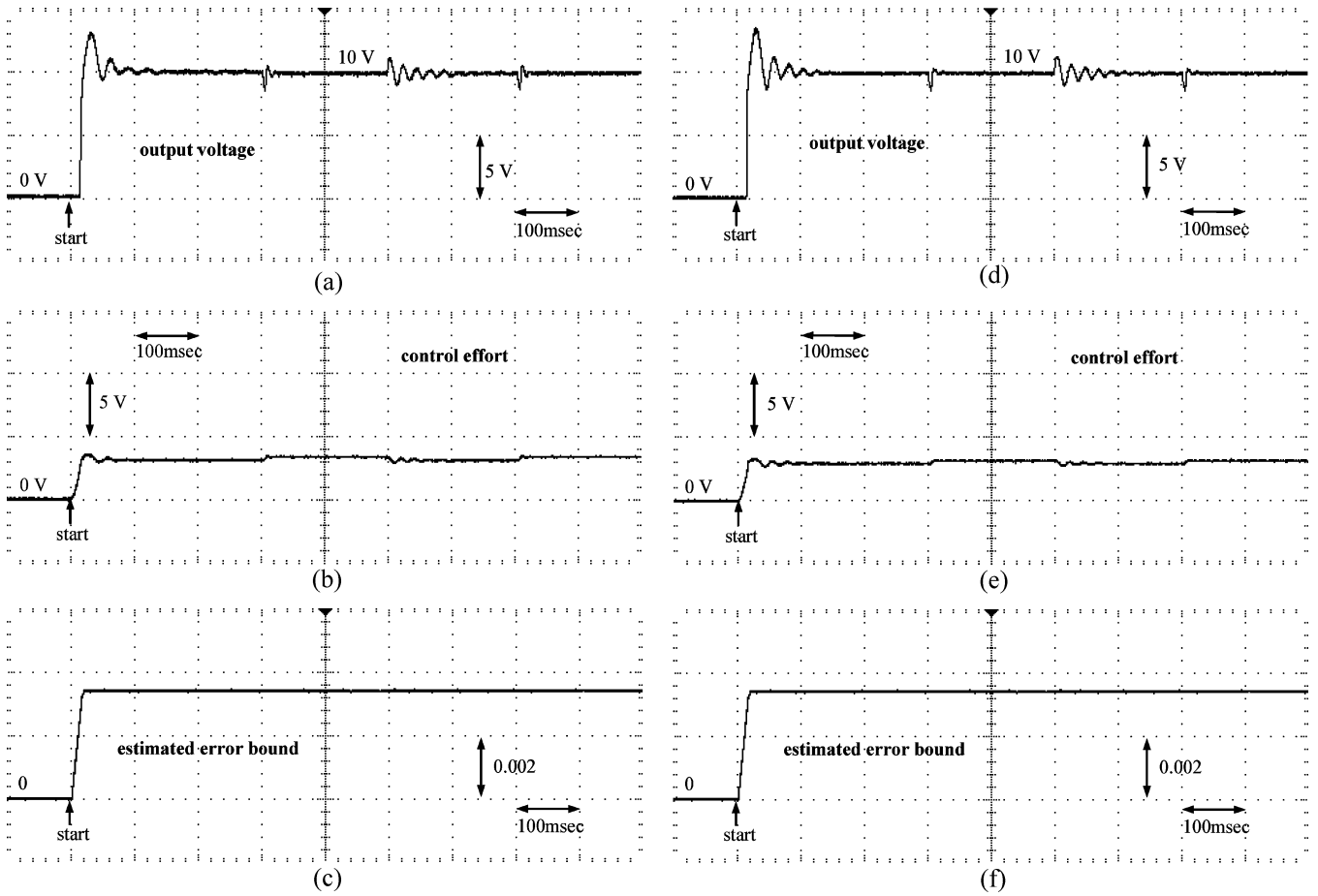

Fig. 6. Experimental results of ANW control with $\eta_\alpha = 0.007$.

where Δe is the output error change and $\Delta\alpha_k^4$ represents the change of weight vector. Using (35) and (40), we get

$$\frac{\partial e(N)}{\partial \alpha_k^4} = \frac{\partial e(N)}{\partial C}\frac{\partial C}{\partial y_o^4}\frac{\partial y_o^4}{\partial net_o^4}\frac{\partial net_o^4}{\partial \alpha_k^4} = -\frac{s}{e(N)}P_\alpha(N). \quad (44)$$

Then (43) becomes

$$e(N+1) = e(N) - \left[\frac{s}{e(N)}P_\alpha(N)\right]^T \eta_\alpha s P_\alpha(N). \quad (45)$$

Thus

$$\begin{aligned}\|e(N+1)\| &= \left\| e(N)\left[1 - \eta_\alpha\left(\frac{s}{e(N)}\right)^2 P_\alpha(N)^T P_\alpha(N)\right]\right\| \\ &\le \|e(N)\|\left\|1 - \eta_\alpha\left(\frac{s}{e(N)}\right)^2 P_\alpha(N)^T P_\alpha(N)\right\|. \quad (46)\end{aligned}$$

From (42) and (46), ΔV_2 can be rewritten as

$$\begin{aligned}\Delta V_2 &= \frac{1}{2}\eta_\alpha s^2 P_\alpha(N)^T P_\alpha(N) \\ &\quad \times \left\{\eta_\alpha\left[\frac{s}{e(N)}\right]^2 P_\alpha(N)^T P_\alpha(N) - 2\right\} \\ &\le \frac{1}{2}\eta_\alpha s^2 (P_{\alpha\max})^2 \\ &\quad \times \left\{\eta_\alpha\left[\frac{s}{e(N)}\right]^2 (P_{\alpha\max})^2 - 2\right\}. \quad (47)\end{aligned}$$

If η_α is chosen as $0 < \eta_\alpha < (2/((P_{\alpha\max})^2[s/e(N)]^2))$, then the Lyapunov stability of $V_2 > 0$ and $\Delta V_2 < 0$ is guaranteed so that the output tracking error will converge to zero as $t \to \infty$. Moreover, the optimal learning-rate which achieves the fast convergence is corresponding to $2\eta_\alpha^*[s/e(N)]^2(P_{\alpha\max})^2 - 2 = 0$, i.e.

$$\eta_\alpha^* = \frac{1}{(P_{\alpha\max})^2\left[\frac{s}{e(N)}\right]^2} \quad (48)$$

which comes from the derivative of (47) with respect to η_α and equals to zero. This shows an interesting result for the variable optimal learning-rate which can be online tuned at each instant.

In summary, the online learning algorithm of the ANW controller is based on the adaptation law (30) for the weight adjustment with the optimal learning-rate in (39). The effectiveness of the adaptive neuro-wavelet control switching power supply can be verified by the following experimental results.

IV. Experimental Results

The block diagram of the computer control system for the converter is depicted in Fig. 4. A servo control card is installed in the control computer, which includes multi-channels of D/A, A/D, PIO, and encoder interface circuits. The proposed ANW control system is realized in the Pentium using the "Visual C" language, and its control interval is set at 40 ms. The amplitude of the dc-link voltage is controlled by the forward switching

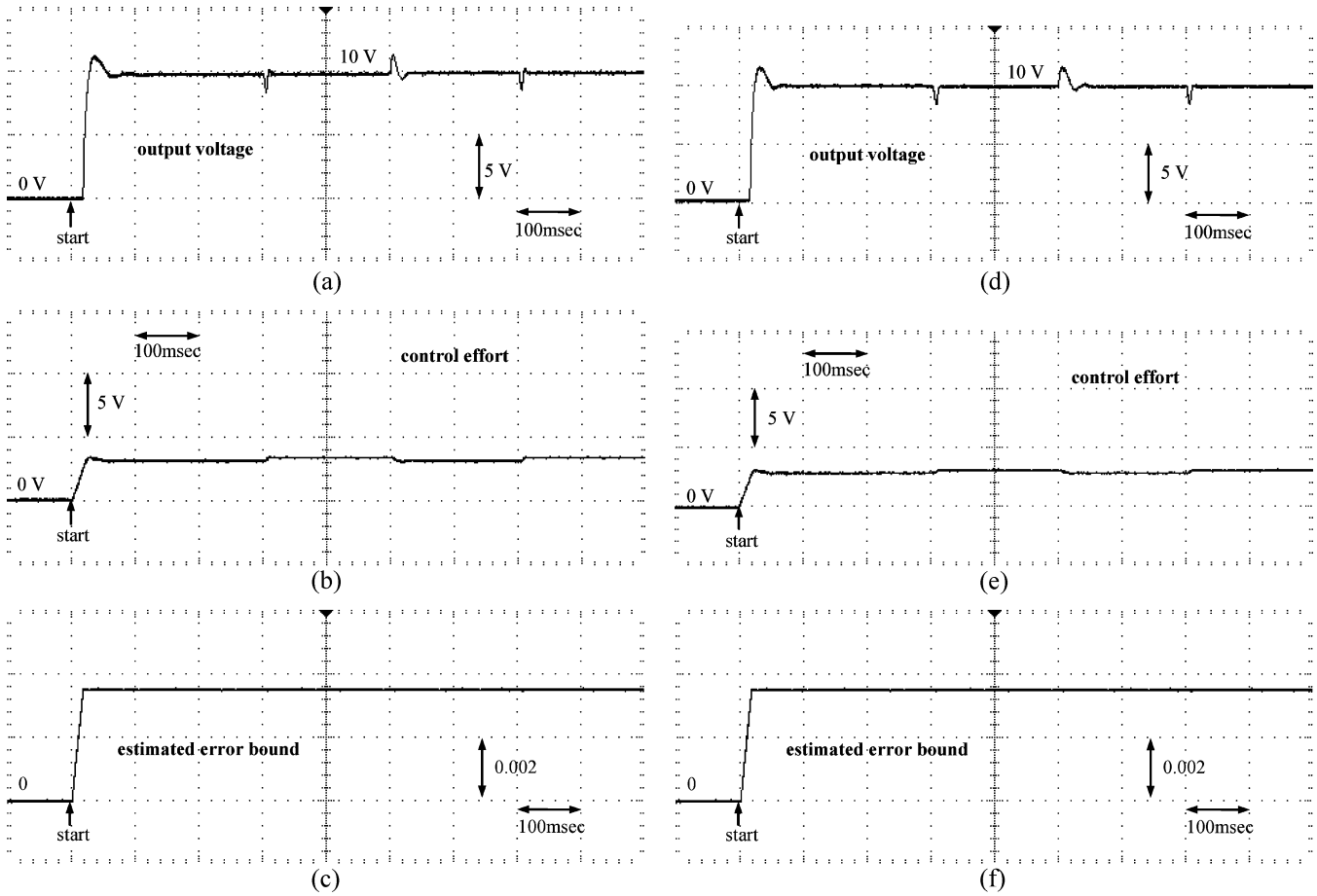

Fig. 7. Experimental results of ANW control with variable optimal learning-rate.

power supply according to the output of the proposed ANN control system. Two experimental cases are addressed as follows: 1) nominal case (the input voltage is set as $V_i = 20$ V) and 2) input variation case (the input voltage is changed to $V_i = 25$ V). In both cases, some load resistance variations with step changes aretested: 1) from 20 Ω to 4 Ω at 300 ms, 2) from 4 Ω to 20 Ω at 500 ms, and 3) from 20 Ω to 4 Ω at 700 ms. The circuit parameter values of the forward dc–dc converter are chosen as $N_1 : N_2 = 4 : 3$, $R = 20\ \Omega$, $L = 500\ \mu$H and $C = 2200\ \mu$F. The converter runs at a switching frequency of 20 KHz and the controller runs at a sampling frequency of 1 KHz. The duty cycle is generated by a PWM IC UC1825; the generated duty cycle is directly proportional to the analog output of the controller. The experiment of the proposed adaptive neuro-wavelet control system is implemented based on the scheme shown in Fig. 2. The input of the wavelet neural network is the tracking index s. The wavelet neural network used in the study can be characterized with the number of elements in layers $n_L = 2$, $n_M = 5$ and $n_N = 25$. In (30), for computing τ, α^* is set as zero at the first experiment. After $\hat{\alpha}$ converges, this convergent value is then used as α^* in the following experiments.

A. ANW Control With Constant Learning-Rates

To illustrate the influence of different learning-rates, first η_α is chosen as a small value. The experimental results of the ANW control with $\eta_\alpha = 0.0005$ for the two cases are shown in Fig. 5. The converter responses are shown in Fig. 5(a) and (d); the associated control efforts are shown in Fig. 5(b) and (e); and the estimated bound $\hat{E}$ are shown in Fig. 5(c) and (f), respectively. To speed up the tracking performance, the experimental results of the ANW control with $\eta_\alpha = 0.007$ for these two cases are shown in Fig. 6. From the experimental results, it can be seen that when a large learning-rate is chosen for achieving fast transient time, the overshoot is relatively large. From the observation, there exists a trade-off between the rise time and the overshoot for the choice of learning-rate. The design of the control parameters must undergo the trail-and-error procedure and the dependency on the expertise experience is unavoidable.

B. ANW Control With Variable Optimal Learning-Rate

The variable optimal learning-rate is used for the ANW control. The experimental results are shown in Fig. 7. Since the learning-rate is automatically tuned, tracking performance is better than that of constant learning-rates. However, since the controller parameters are initialized from zero, the ANW control has the drawback of large overshoot at the initial learning phase. After training, the trained ANW control is applied to control the forward switching power supply again. The experimental results of the trained ANW control system for these two cases are shown in Fig. 8. From the experimental results, it is seen that the regulation performance of the trained ANW control is further improved when the initial values are trained, and they can achieve favorable robust characteristics for the load variations.

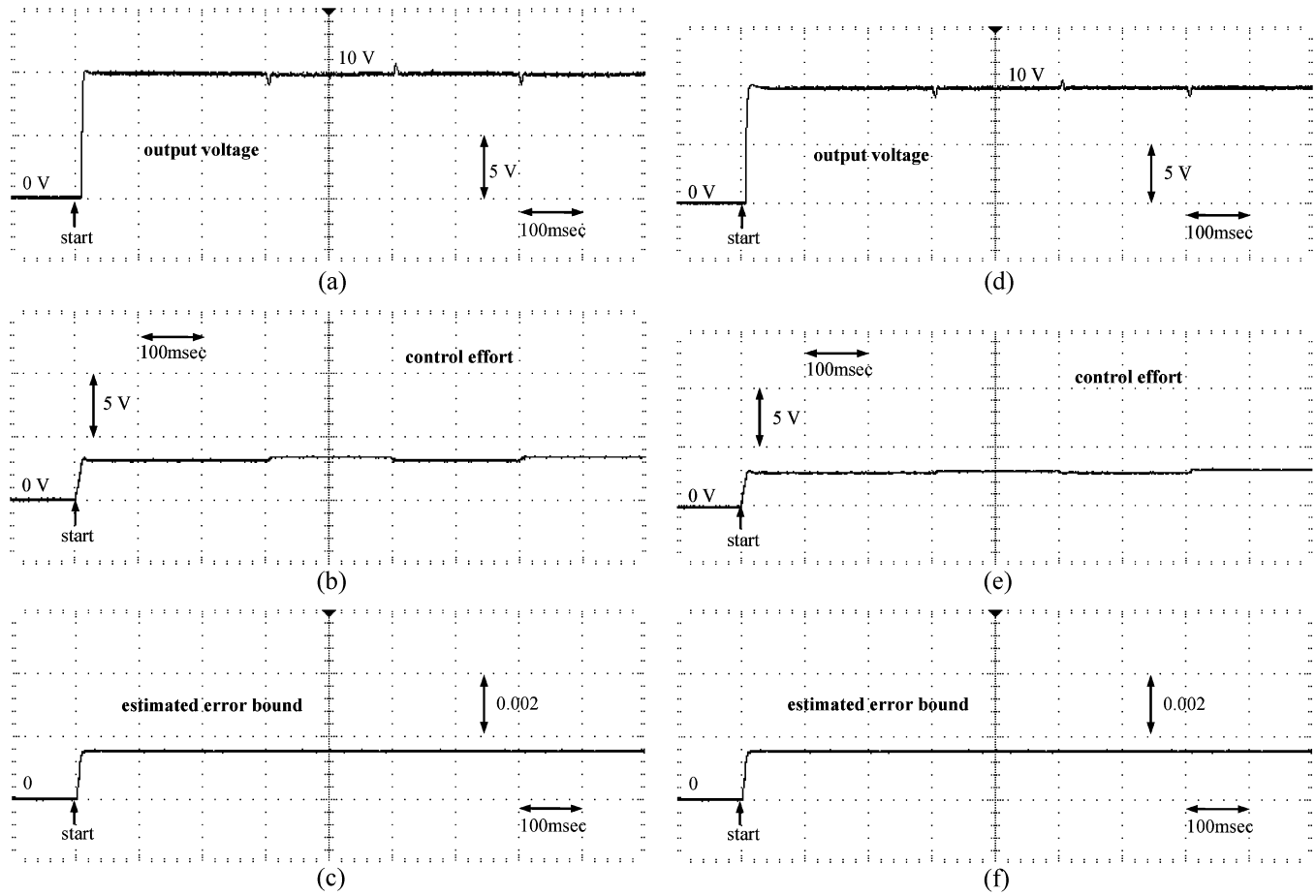

Fig. 8. Experimental results of trained ANW control with variable optimal learning-rate.

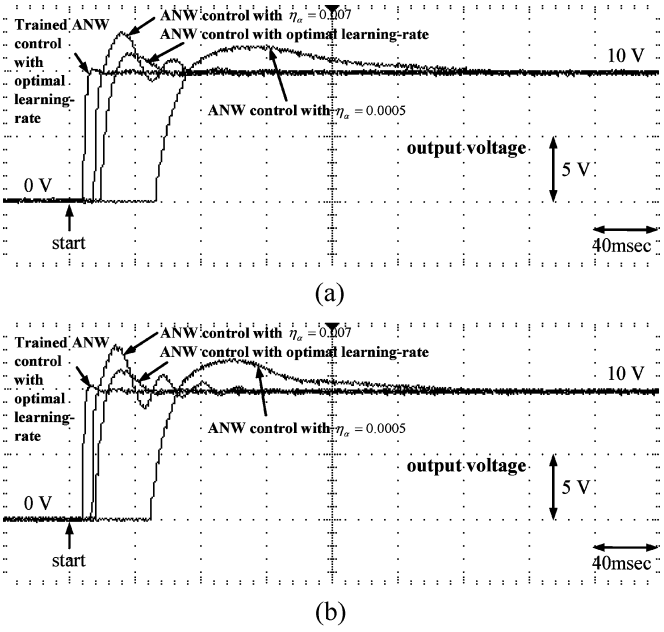

Fig. 9. Transient response comparison.

A transient response comparison among these experiments is shown in Fig. 9. After the ANW control has been sufficiently trained by the developed learning algorithm, the trained ANW control demonstrates a remarkable performance in voltage stabilization, all in rise time, settling time, overshoot and load variation regulations. In conclusion, the trained ANW control can achieve better performance than the other ones.

V. Conclusion

This paper has successfully implemented an ANW control for a forward switching power supply. The effectiveness of the proposed ANW control is verified by various experimental results. From the experimental results, the output voltage of the forward switching power supply can be maintained to follow the desired output voltage with favorable transient response and regulation performance. The major contributions of this paper are: 1) the successful development of an ANW control system in which the Lyapunov stability theorem is used to online tune the parameters, 2) the successful development of an online training methodology with variable optimal learning-rate for the ANW control system, 3) a computer-based experiment setup has been created, and 4) the successful application of the ANW to control the forward switching power supply.

References

[1] O. Omidvar and D. L. Elliott, *Neural Systems for Control*. New York: Academic, 1997.

[2] S. Seshagiri and H. K. Khalil, "Output feedback control of nonlinear systems using RBF neural networks," *IEEE Trans. Neural Netw.*, vol. 11, no. 1, pp. 69–79, Jan. 2000.

[3] C. H. Wang, H. L. Liu, and T. C. Lin, "Direct adaptive fuzzy-neural control with state observer and supervisory controller for unknown nonlinear dynamical systems," *IEEE Trans. Fuzzy Syst.*, vol. 10, no. 1, pp. 39–49, Feb. 2002.
[4] C. M. Lin and C. F. Hsu, "Neural network hybrid control for antilock braking systems," *IEEE Trans. Neural Network*, vol. 14, no. 2, pp. 351–359, Mar. 2003.
[5] C. F. Hsu, C. M. Lin, and T. Y. Chen, "Neural-network-identification-based adaptive control of wing rock motion," *Proc. Inst. Elect. Eng.*, vol. 152, pp. 65–71, Jan. 2005.
[6] B. Delyon, A. Juditsky, and A. Benveniste, "Accuracy analysis for wavelet approximations," *IEEE Trans. Neural Netw.*, vol. 6, no. 2, pp. 332–348, Mar. 1995.
[7] Q. Zhang, "Using wavelet network in nonparametric estimation," *IEEE Trans. Neural Networks*, vol. 8, no. 2, pp. 227–236, Mar. 1997.
[8] D. W. C. Ho, P. A. Zhang, and J. Xu, "Fuzzy wavelet networks for function learning," *IEEE Trans. Fuzzy Syst.*, vol. 9, no. 1, pp. 200–211, Feb. 2001.
[9] C. K. Lin, "Adaptive tracking controller design for robotic systems using Gaussian wavelet networks," *Proc. Inst. Elect. Eng.*, vol. 149, pp. 316–322, Jul. 2002.
[10] C. D. Sousa, E. M. Hemerly, and R. K. H. Galvao, "Adaptive control for mobile robot using wavelet networks," *IEEE Trans. Syst., Man Cybern. B*, vol. 32, no. 4, pp. 493–504, Aug. 2002.
[11] C. L. Lin, N. C. Shieh, and P. C. Tung, "Robust wavelet neuro control for linear brushless motors," *IEEE Trans. Aerosp. Electron. Syst.*, vol. 38, no. 3, pp. 918–932, Jul. 2002.
[12] R. J. Wai, "Development of new training algorithms for neuro-wavelet systems on the robust control of induction servo motor drive," *IEEE Trans. Ind. Electron.*, vol. 49, no. 6, pp. 1323–1341, Dec. 2002.
[13] R. D. Middlebrook and S. Cuk, *Advances in Switched-Mode Power Conversion*. Pasadena, CA: Teslaco, 1981.
[14] A. I. Pressman, *Switching Power Supply Design*. New York: McGraw-Hill, 1998.
[15] J. Alvarez-Ramirez, I. Cervantes, G. Espinosa-Perez, P. Maya, and A. Morales, "A stable design of PI control for DC-DC converters with an RHS zero," *IEEE Trans. Circuits Syst. I*, vol. 48, no. 1, pp. 103–106, Jan. 2001.
[16] F. H. Hsieh, N. Z. Yen, and Y. T. Juang, "Optimal controller of a buck DC-DC converter using the uncertain load as stochastic noise," *IEEE Trans. Circuits Syst. II*, vol. 52, no. 2, pp. 77–81, Feb. 2005.
[17] E. Vidal-Ldiarte, L. Martine-Salamero, F. Guinjoan, J. Calvente, and S. Gomariz, "Sliding and fuzzy control of a boot converter using an 8-bit microcontroller," *Proc. Inst. Elect. Eng.*, vol. 151, pp. 5–11, Jan. 2004.
[18] M. Lopez, L. G. Vicuna, M. Castilla, P. Gaya, and O. Lopez, "Current distribution control design for paralleled DC/DC converters using sliding-mode control," *IEEE Trans. Ind. Electron.*, vol. 51, no. 2, pp. 419–428, Apr. 2004.
[19] A. Balestrino, A. Landi, and L. Sani, "Cuk converter global control via fuzzy logic and scaling factors," *IEEE Trans. Ind. Appl.*, vol. 38, no. 2, pp. 406–413, Mar.Apr. 2002.
[20] M. A. Mayosky and G. I. E. Cancelo, "Direct adaptive control of wind energy conversion system using Gaussian network," *IEEE Trans. Neural Netw.*, vol. 10, no. 4, pp. 898–906, Jul. 1999.
[21] L. X. Wang, *Adaptive Fuzzy Systems and Control: Design and Stability Analysis*. Englewood Cliffs, NJ: Prentice-Hall, 1994.
[22] S. Sastry and M. Bodson, *Adaptive Control—Stability, Convergence, and Robustness*. Englewood Cliffs, NJ: Prentice-Hall, 1989.

Chih-Min Lin (S'86–M'87–SM'99) was born in Taiwan, R.O.C., in 1959. He received the B. S. and M. S. degrees in control engineering and the Ph.D. degree in electronics engineering from National Chiao Tung University, Hsinchu, Taiwan, R.O.C., in 1981, 1983, and 1986, respectively.

He joined the faculty of the Department of Electrical Engineering, Yuan-Ze University, Taoyuan, Taiwan, in 1993 and is currently a Professor and the Chairman of the Department of Electrical Engineering. From 1997 to 1998, he was the Honor Research Fellow with the University of Auckland, New Zealand. His research interests include fuzzy neural networks, cerebellar model articulation control, guidance and flight control, and systems engineering.

Dr. Lin was a Committee Member of the Chinese Automatic Control Society and the Deputy Chairman of the IEEE Control Systems Society, Taipei Section.

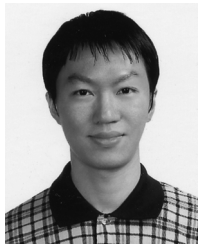

Kun-Neng Hung was born in Taiwan, R.O.C., in 1982. He received the B. S. degrees in electrical engineering from Yuan Ze University, Taoyuan, Taiwan, R.O.C., in 2004 where he is currently pursuing the M. S. degree in electrical engineering.

His research interests include switching power supply and intelligent control.

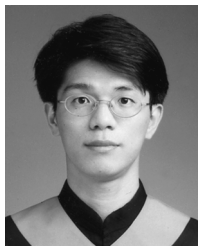

Chun-Fei Hsu (M'05) received the B. S., M.S., and Ph.D. degrees in electrical engineering from Yuan-Ze University, Taoyuan, Taiwan, R.O.C., in 1997, 1999, and 2002, respectively.

After graduation, he joined the Department of Electrical and Control Engineering, National Chiao-Tung University, Hsinchu, Taiwan, where he is currently engaged in postdoctoral work. His research interests include power electronics, servomotor drives and intelligent control using fuzzy systems and neural network technologies.